Inorg. Chem. **2008**, *47*, 2805−2810

Inorganic Chemistry
Article

Visible Light-Driven Electron Transfer and Hydrogen Generation Catalyzed by Bioinspired [2Fe2S] Complexes

Yong Na,[†] Mei Wang,[*,†] Jingxi Pan,[†] Pan Zhang,[†] Björn Åkermark,[‡] and Licheng Sun[*,†,§]

State Key Laboratory of Fine Chemicals, DUT-KTH Joint Education and Research Centre on Molecular Devices, Dalian University of Technology (DUT), 116012 Dalian, China, Department of Organic Chemistry, Arrhenius Laboratory, Stockholm University, 10691 Stockholm, Sweden, and Department of Chemistry, Royal Institute of Technology (KTH), Teknikringen 30, 10044, Stockholm, Sweden

Received October 11, 2007

Complexes $[\{(\mu\text{-SCH}_2)_2\text{NCH}_2\text{C}_6\text{H}_5\}\{\text{Fe(CO)}_2\text{L}^1\}\{\text{Fe(CO)}_2\text{L}^2\}]$ (L^1 = CO, L^2 = P(Pyr)$_3$, **2**; $L^1 = L^2$ = P(Pyr)$_3$, **3**) were prepared, which have the lowest reduction potentials for the mono- and double-CO-displaced diiron complexes reported so far. Hydrogen evolution, driven by visible light, was successfully observed for a three-component system, consisting of a ruthenium polypyridine complex, the biomimetic model complex **2** or **3**, and ascorbic acid as both electron and proton donor in CH_3CN/H_2O. The electron transfer from photogenerated $Ru(bpy)_3^+$ to **2** or **3** was detected by laser flash photolysis. Under optimal conditions, the total turnover number for hydrogen evolution was 4.3 based on **2** and 86 based on $Ru(bpy)_3^{2+}$ in a three-hour photolysis.

Introduction

Hydrogen is known as a clean fuel and a promising alternative to fossil fuels, which in addition to being in limited supply have well-known detrimental effects on the environment. Conversion of solar energy into hydrogen is a challenging task and has attracted extensive attention during recent decades.[1,2] Numerous studies on photochemical hydrogen evolution by visible light-driven water splitting have been reported since the late 1970s.[3–6] While heterogeneous photocatalysis by multiple components has been extensively studied,[7–10] there are relatively few reports on homogeneous catalysts for the light-driven hydrogen production.[11–18] Almost in all cases, either with hetero or homogeneous catalyst systems, noble metal-based (Pt, Rh, Pd, etc.) compounds were used as catalysts. Inspired by the remark-

---

[*] To whom correspondence should be addressed. E-mail: symbueno@dlut.edu.cn.

[†] Dalian University of Technology.

[‡] Stockholm University.

[§] Royal Institute of Technology.

(1) Service, R. F. *Science* **2005**, *309*, 548–551.
(2) Eisenberg, R.; Nocera, D. G. *Inorg. Chem.* **2005**, *44*, 6799–6801.
(3) Lehn, J.-M.; Sauvage, J.-P. *Nouv. J. Chim.* **1977**, *1*, 449–451.
(4) Kalyanasundaram, K.; Kiwi, J.; Grätzel, M. *Helv. Chim. Acta* **1978**, *61*, 2720–2730.
(5) Moradpour, A.; Amouyal, E.; Keller, P.; Kagan, H. *Nouv. J. Chim.* **1978**, *2*, 547–549.
(6) Kirch, M.; Lehn, J.-M.; Sauvage, J.-P. *Helv. Chim. Acta* **1979**, *62*, 1345–1384.
(7) Lehn, J.-M.; Sauvage, J.-P.; Ziessel, R. *Nouv. J. Chim.* **1981**, *5*, 291–295.
(8) Grätzel, M. *Acc. Chem. Res.* **1981**, *14*, 376–384.
(9) Bard, A. J.; Fox, M. A. *Acc. Chem. Res.* **1995**, *28*, 141–145.
(10) Kim, Y. I.; Keller, S. W.; Krueger, J. S.; Yonemoto, E. H.; Saupe, G. B.; Mallouk, T. E. *J. Phys. Chem. B* **1997**, *101*, 2491–2500.
(11) Brown, G. M.; Brunschwig, B. S.; Creutz, C.; Endicott, J. F.; Sutin, N. *J. Am. Chem. Soc.* **1979**, *101*, 1298–1300.
(12) Krishnan, C. V.; Sutin, N. *J. Am. Chem. Soc.* **1981**, *103*, 2141–2142.
(13) Fisher, J. R.; Cole-Hamilton, D. J. *J. Chem. Soc., Dalton Trans.* **1984**, 809–813.
(14) Krishnan, C. V.; Brunschwig, B. S.; Creutz, C.; Sutin, N. *J. Am. Chem. Soc.* **1985**, *107*, 2005–2015.
(15) Goldsmith, J. I.; Hudson, W. R.; Lowry, M. S.; Anderson, T. H.; Bernhard, S. *J. Am. Chem. Soc.* **2005**, *127*, 7502–7510.
(16) Ozawa, H.; Haga, M.; Sakai, K. *J. Am. Chem. Soc.* **2006**, *128*, 4926–4927.
(17) Rau, S.; Schäfer, B.; Gleich, D.; Anders, E.; Rudolph, M.; Friedrich, M.; Görls, H.; Henry, W.; Vos, J. G. *Angew. Chem., Int. Ed.* **2006**, *45*, 6215–6218.
(18) Kimura, E.; Bu, X.; Shionoya, M.; Wada, S.; Maruyama, S. *Inorg. Chem.* **1992**, *31*, 4542–4546.
(19) Frey, M. *ChemBioChem.* **2002**, *3*, 153–160.
(20) Gloaguen, F.; Lawrence, J. D.; Rauchfuss, T. B. *J. Am. Chem. Soc.* **2001**, *123*, 9476–9477.
(21) Borg, S. J.; Behrsing, T.; Best, S. P.; Razavet, M.; Liu, X.; Pickett, C. J. *J. Am. Chem. Soc.* **2004**, *126*, 16988–16999.
(22) Capon, J.-F.; Gloaguen, F.; Schollhammer, P.; Talarmin, J. *Coord. Chem. Rev.* **2005**, *249*, 1664–1676.
(23) Chong, D.; Georgakaki, I. P.; Mejia-Rodriguez, R.; Sanabria-Chinchilla, J.; Soriaga, M. P.; Darensbourg, M. Y. *Dalton Trans.* **2003**, 4158–4163.
(24) Mejia-Rodriguez, R.; Chong, D.; Reibenspies, J. H.; Soriaga, M. P.; Darensbourg, M. Y. *J. Am. Chem. Soc.* **2004**, *126*, 12004–12014.
(25) Sun, L.; Åkermark, B.; Ott, S. *Coord. Chem. Rev.* **2005**, *249*, 1653–1663.

10.1021/ic702010w CCC: $40.75

able catalytic activity (6000–9000 molecules H_2 s^{-1} per site) of Fe-Fe hydrogenases ([FeFe]H_2ase) for proton reduction to H_2,[19] many chemists are engaged in creating electro- and photochemical hydrogen production catalyst systems based on the diiron model complexes of the [FeFe]H_2ase active site.[20–25]

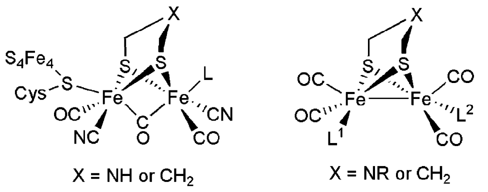

(a) [FeFe]H_2ase active site (b) model complexes

The first example for electrocatalytic proton reduction based on the bioinspired diiron dithiolate complex $[\{(\mu\text{-}SCH_2)_2CH_2\}\{Fe(CO)_2PMe_3\}\{Fe(CO)_2CN\}]^-$ was reported with six turnovers by Rauchfuss and co-workers in 2001.[20] In the following years, many biomimetic diiron complexes were found electrocatalytically active for proton reduction to H_2 with ca. 0.5−1.0 V overpotential in the presence of weak acid (HOAc) in CH_3CN,[23,24,26–28] and with relatively large overpotential (ca. 0.75−1.22 V) in the presence of moderate and strong acids (HOTs, $HBF_4 \cdot Et_2O$, H_2SO_4, and $HClO_4$) in CH_3CN with the maximum turnovers of 25.[20–22,29,30] While a number of synthetic diiron dithiolate complexes have been widely studied for electrochemical hydrogen production, catalysts based on bioinspired diiron complexes for photochemical hydrogen production have not been reported so far.

Ruthenium polypyridine complexes have been successfully used as a light harvesting unit in many light-driven hydrogen production systems.[3–14,31,32] To build intramolecular photoinduced catalysts, several biomimetic models of the [FeFe]H_2ase active site were covalently linked to the ruthenium photosensitizer or to the porphyrin derivative.[25,33] However, the diiron catalytic center cannot be directly reduced by the excited photosensitizer, which was quenched either by energy transfer or by unwanted reverse electron transfer.[34] It is mainly because the reduction potential of the dinuclear iron complex is more negative than the oxidation potential of the excited-state of the ruthenium complex, making the direct electron transfer from the excited photosensitizer to the catalyst thermodynamically unfavorable. To overcome this problem, a stronger reductant $Ru(bpy)_3^+$, which can be generated via reductive quenching of the excited-state of $Ru(bpy)_3^{2+}$, might possess enough driving force for the desired electron transfer reaction.[35]

We have recently demonstrated that the $Ru(bpy)_3^+$, photogenerated via a reductive quenching using diethyldithiocarbamate anion (dtc^-) as an electron donor, could transfer one electron to the diiron dithiolate complexes $[\{(\mu\text{-}SCH_2)_2X\}\{Fe(CO)_3\}_2]$ (X = CH_2, $NCH_2C_6H_5$),[36] resulting in the formation of Fe^0Fe^I species. Such species are proposed to be crucial intermediates in electrochemical hydrogen evolution catalyzed by [2Fe2S] complexes.[21–24,26–28] The three-component system of $Ru(bpy)_3^{2+}$, all-CO diiron complex and dtc^- has two shortcomings for photochemical hydrogen generation. First, the all-CO diiron complexes are gradually decomposed under long time irradiation. To improve the photostability of the [2Fe2S] model complex, phosphine-coordinated complexes could be considered as catalyst candidates, but CO-displacement by common phosphine ligands results in a great cathodic shift of reduction potentials for [2Fe2S] complexes,[24,26,37,38] which makes electron transfer from $Ru(bpy)_3^+$ to Fe^IFe^I species thermodynamically unfavorable. Therefore we prepared diiron complexes containing weak electron donating phosphine ligand(s), tris(*N*-pyrrolyl)phosphine ($P(Pyr)_3$),[39] and used them as catalysts for photochemical hydrogen production. Second, the ionic quencher dtc^- is protonated and decomposed in the presence of proton acid. To overcome this problem, an acid-tolerant quencher should be used to replace the S-containing electron donor. Ascorbic acid (H_2A) is a good candidate since it can act as a proton source and its ascorbate anion (HA^-) can function as reductive quencher for $^*Ru(bpy)_3^{2+}$ to $Ru(bpy)_3^+$.[11] Here we present the results on photoinduced electron transfer and light-driven hydrogen generation using a three-component catalytic system of $Ru(bpy)_3^{2+}$, H_2A, and $[\{(\mu\text{-}SCH_2)_2NCH_2C_6H_5\}\{Fe(CO)_2L^1\}\{Fe(CO)_2L^2\}]$ ($L^1 = L^2 =$ CO, **1**; $L^1 =$ CO, $L^2 = P(Pyr)_3$, **2**; $L^1 = L^2 = P(Pyr)_3$, **3**) (Scheme 1).

Experimental Section

Reagents and Instruments. All reactions were carried out under N_2 atmosphere with standard Schlenk techniques. Solvents were dried and distilled prior to use according to the standard methods. 4,4′-Dimethyl-2,2′-bipyridyl (dmbpy) and 2,2′-bipyridyl (bpy) were purchased from Aldrich and used as received. Photosensitizers $[Ru(bpy)_3](PF_6)_2$, $[Ru(dmbpy)(bpy)_2](PF_6)_2$, and $[Ru(dmbpy)_3](PF_6)_2$ were synthesized according to the literature procedures.[40,41]

---

(26) Na, Y.; Wang, M.; Jin, K.; Zhang, R.; Sun, L. *J. Organomet. Chem.* **2006**, *691*, 5045–5051.
(27) Duan, L.; Wang, M.; Li, P.; Na, Y.; Wang, N.; Sun, L. *Dalton Trans.* **2007**, *1277*, 1283.
(28) Felton, G. A. N.; Vannucci, A. K.; Chen, J.; Lockett, L. T.; Okumura, N.; Petro, B. J.; Zakai, U. I.; Evans, D. H.; Glass, R. S.; Lichtenberger, D. L. *J. Am. Chem. Soc.* **2007**, *129*, 12521–12530.
(29) Ott, S.; Kritikos, M.; Åkermark, B.; Sun, L.; Lomoth, R. *Angew. Chem., Int. Ed.* **2004**, *43*, 1006–1009.
(30) Capon, J.-F.; Gloaguen, F.; Schollhammer, P.; Talarmin, J. *J. Electroanal. Chem.* **2006**, *595*, 47–52.
(31) Rau, S.; Walther, D.; Vos, J. G. *Dalton Trans.* **2007**, 915–919.
(32) Okura, I.; Nakamura, S.; Kim-Thuan, N.; Nakamura, K.-I. *J. Mol. Catal.* **1979**, *6*, 261–267.
(33) Song, L.-C.; Tang, M.-Y.; Su, F.-H.; Hu, Q.-M. *Angew. Chem., Int. Ed.* **2006**, *45*, 1130–1133.
(34) Eksröm, J.; Abrahamsson, M.; Olson, C.; Bergquist, J.; Kaynak, F. B.; Eriksson, L.; Sun, L.; Becker, H.-C.; Åkermark, B.; Hammarström, L.; Ott, S. *Dalton Trans.* **2006**, 4599–4606.
(35) Balzani, V.; Bergamini, G.; Marchioni, F.; Ceroni, P. *Coord. Chem. Rev.* **2006**, *250*, 1254–1266.
(36) Na, Y.; Pan, J.; Wang, M.; Sun, L. *Inorg. Chem.* **2007**, *46*, 3813–3815.
(37) Li, P.; Wang, M.; He, C.; Li, G.; Liu, X.; Chen, C.; Åkermark, B.; Sun, L. *Eur. J. Inorg. Chem.* **2005**, 2506–2513.
(38) Wang, F.; Wang, M.; Liu, X.; Jin, K.; Dong, W.; Sun, L. *Dalton Trans.* **2007**, 3812–3819.
(39) Jackstell, R.; Klein, H.; Beller, M.; Wiese, K.-D.; Röttger, D. *Eur. J. Org. Chem.* **2001**, 3871–3877.
(40) Thummel, R. P.; Lefoulon, F. *Inorg. Chem.* **1987**, *26*, 675–680.
(41) Orellana, G.; Quiroga, M. L.; Braun, A. M. *Helv. Chim. Acta* **1987**, *70*, 2073–2086.

Scheme 1. The Homogeneous Molecular Three-Component System for Photochemical H_2 Generation Catalysed by [FeFe]H_2ase Active Site Mimics

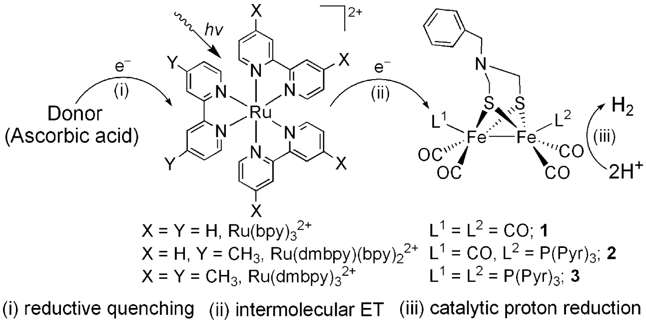

Complex [{(μ-SCH_2)$_2$N($CH_2C_6H_5$)}$Fe_2(CO)_6$] (**1**) was synthesized as previously reported.[36] Tris(*N*-pyrrolyl)phosphine (P(Pyr)$_3$) was prepared by following the literature protocol.[39]

IR spectra were recorded in $CHCl_3$ on a JASCO FT/IR 430 spectrophotometer. ^1H and ^{31}P NMR spectra were recorded on a Varian INOVA 400NMR instrument. Mass spectra were recorded on an HP1100 MSD instrument. Elemental analyses were performed on a VarioEL III elemental analyzer.

[{(μ-SCH_2)$_2$$NCH_2C_6H_5$}{$Fe(CO)_3$}{$Fe(CO)_2P(Pyr)_3$}] (2). The CO-removing reagent $Me_3NO\cdot 2H_2O$ (56 mg, 0.5 mmol) was added to the solution of complex **1** (240 mg, 0.5 mmol) in CH_3CN (20 mL), and the mixture was stirred at room temperature for 10 min. Ligand P(Pyr)$_3$ (115 mg, 0.5 mmol) was added to the mixture. The reaction solution was refluxed for 6 h. After solvent was removed on a rotary evaporator, the crude product was purified by column chromatography on silica gel with hexane/CH_2Cl_2 (4:1, v/v) as eluent. The product was obtained in a yield of 260 mg (76%). Anal. Calcd for $C_{26}H_{23}N_4O_5PS_2Fe_2$: C, 46.04; H, 3.42; N, 8.26. Found: C, 46.21; H, 3.41; N, 8.37%. ^1H NMR ($CDCl_3$): δ 2.28 (s, 2H, SCH_2), 2.99 (s, 2H, SCH_2), 3.18 (s, 2H, $PhCH_2N$), 6.31 (s, 6H, pyrrolyl), 6.83 (s, 6H, pyrrolyl), 6.90 (s, 1H, Ph), 7.18 (s, 4H, Ph). $^{31}P\{^1H\}$ NMR: δ 141.19. IR ($CHCl_3$): υ_{CO} 2055 (s), 2002 (s), 1983 (s) cm^{-1}. MS (API-ES): *m/z*: 678.9 $[M + H]^+$.

[{(μ-SCH_2)$_2$$NCH_2C_6H_5$}{$Fe(CO)_2P(Pyr)_3$}$_2$] (3). Ligand P(Pyr)$_3$ (68 mg, 0.3 mmol) was added to the solution of complex **2** (102 mg, 0.15 mmol) in toluene (50 mL), and the mixture was refluxed for 20 h. As solvent was evaporated under reduced pressure, the product was purified by column chromatography on silica gel first with hexane/CH_2Cl_2 (4:1, v/v) and then with hexane/CH_2Cl_2 (3:1, v/v) as eluents. The product was obtained in a yield of 86 mg (65%). Anal. Calcd for $C_{37}H_{35}N_7O_4P_2S_2Fe_2$: C, 50.53; H, 4.01; N, 11.15. Found: C, 50.58; H, 3.95; N, 11.25%. ^1H NMR ($CDCl_3$): δ 2.16 (s, 4H, SCH_2), 2.69 (s, 2H, $PhCH_2N$), 6.26 (s, 12H, pyrrolyl), 6.49 (d, 2H, Ph), 6.81 (s, 12H, pyrrolyl), 7.05 (m, 3H, Ph). $^{31}P\{^1H\}$ NMR: δ 138.27. IR ($CHCl_3$): υ(CO) 2025 (s), 1983 (m), 1968 (s) cm^{-1}. MS (API-ES): *m/z*: 880.0 $[M + H]^+$.

Electrochemistry. Electrochemistry measurements were recorded using a BAS-100W electrochemical potentiostat at a scan rate of 100 mV/s. Cyclic voltammogram experiments were performed in a three-electrode cell under argon. The working electrode was a glassy carbon disk (diameter, 3 mm) polished with 1-μm diamond paste and sonicated for 15 min prior to use, and the auxiliary electrode was a platinum wire. The reference electrode was an Ag/Ag^+ electrode (0.01 M $AgNO_3$ in CH_3CN). A solution of 0.05 M *n*-Bu_4NPF_6 in CH_3CN or a mixture of 0.05 M *n*-Bu_4NPF_6 in CH_3CN and 0.05 M KCl in water were used as electrolyte. The electrolyte solution was degassed by bubbling with dry argon for 10 min before measurement. All potentials are versus Ag/Ag^+ (0.01 M $AgNO_3$ in CH_3CN).

Laser Flash Photolysis. Nanosecond transient absorption measurements were performed on a LP-920 pump–probe spectroscopic setup (Edinburgh). The excitation source was the unfocused third harmonic (532 nm, 7 ns fwhm) output of a Nd:YAG laser (Continuum surelite II), and the probe light source was a pulse-xenon lamp. The signals were detected by Edinburgh analytical instruments (LP900) and recorded on a Tektronix TDS 3012B oscilloscope and computer. All samples in flash photolysis experiments were deaerated with argon for ca. 20 min.

Photocatalysis. In a typical experiment, $[Ru(bpy)_3](PF_6)_2$ (0.86 mg, 1 μmol), H_2A (176 mg, 1 mmol), complex **2** (6.8 mg, 10 μmol) and CH_3CN (5 mL) were added to a Schlenk tube. Water (5 mL) was added after the mixture was stirred under N_2 atmosphere for 5 min. The suspension was then stirred for another 10 min until H_2A was completely dissolved. The solution was freeze–pump–thaw degassed for three times and then warmed to room temperature prior to irradiation. The Schlenk tube was connected to a small balloon of pure N_2 with an atmospheric pressure. The gas phase volume is 59 mL, and the total amount of hydrogen gas evolved in the photocatalytic reaction is no more than 1 mL. The reaction solution was irradiated at 25 °C using an Xe lamp (500 W) with a Pyrex-glass filter ($\lambda >$ ca. 400 nm). The gas phase of the reaction system was analyzed on a GC 7890T instrument with a thermal conductivity detector, a 5 Å molecular sieve column, and with N_2 as carrying gas. The amount of hydrogen evolved was determined by the external standard method. Hydrogen in the resulting solution was not measured and the slight effect of the hydrogen gas evolved on the pressure inside the Schlenk tube was neglected for calculation of the volume of hydrogen gas.

Results and Discussion

Preparation of Complexes 2 and 3. In the presence of CO-removing reagent $Me_3NO\cdot 2H_2O$, the reaction of equivalent of **1** and P(Pyr)$_3$ gave monosubstituted diiron complex **2** in a good yield. Further CO-displacement of **2** with excess P(Pyr)$_3$ in refluxing toluene afforded disubstituted complex **3** in moderate yield. Complexes **2** and **3** were characterized by MS, IR, ^1H and ^{31}P NMR spectra and elemental analysis. The results of the mass spectra and the elemental analyses for **2** and **3** are in good agreement with the supposed diiron complexes. Each complex displays three υ_{CO} bands as those reported for other analogous PR_3-mono and -disubstituted diiron complexes.[24,26,37,38] The υ_{CO} bands of P(Pyr)$_3$-monosubsituted complex **2** display an average red shift of 17 cm^{-1} in comparison to that for the parent all-CO diiron complex **1**,[36] and the υ_{CO} bands of P(Pyr)$_3$-disubstituted complex **3** show a further 21 cm^{-1} shift to lower frequencies. The average red shifts for υ_{CO} bands of complexes **2** and **3** are much smaller than those for the analogous PR_3- (PMe_3, $P(OEt)_3$, PTA (1,3,5-triaza-7-phosphaadamantane)) mono- and disubstituted diiron complexes reported previously (Table 1),[24,37,42] indicating the relatively weak electron donating properties of the P(Pyr)$_3$ ligand in comparison with those of other PR_3-coordinated diiron complexes described above.

Electrochemistry. Diiron complexes **2** and **3** display the Fe^IFe^I/Fe^0Fe^I reduction events at –1.52 and –1.55 V in CH_3CN, respectively, which are the lowest reduction potentials for the mono- and double-CO-displaced diiron dithiolate

---

(42) Eilers, G.; Schwartz, L.; Stein, M.; Zampella, G.; de Dioia, L.; Ott, S.; Lomoth, R. *Chem. Eur. J.* **2007**, *13*, 7075–7084.

Table 1. A Comparison of the $\Delta\nu_{CO}$ and ΔE Values of **2** and **3** with Those of Other PR_3-Coordinated Diiron Complexes[a]

complex	$\Delta\nu_{CO}$ cm^{-1}	ΔE mV	note
$[\{(\mu\text{-}SCH_2)_2NCH_2C_6H_5\}Fe_2(CO)_5P(Pyr)_3]$ (**2**)	17	30	this work
$[(\mu\text{-pdt})Fe_2(CO)_5PMe_3]$	56	290	ref 37
$[(\mu\text{-pdt})Fe_2(CO)_5PTA]$	52	200	ref 24
$[(\mu\text{-pdt})Fe_2(CO)_5P(OEt)_3]$	45	160	ref 37
$[\{(\mu\text{-}SCH_2)_2NCH_2C_6H_5\}\{Fe(CO)_2P(Pyr)_3\}_2]$ (**3**)	38	70	this work
$[\{(\mu\text{-}SCH_2)_2NCH_2C_6H_5\}\{Fe(CO)_2PMe_3\}_2]$	95	620	ref 42
$[(\mu\text{-pdt})\{Fe(CO)_2PMe_3\}_2]$	95	510	ref 24
$[(\mu\text{-pdt})\{Fe(CO)_2PTA\}_2]$	86	440	ref 24

[a] $\Delta\nu_{CO} = \nu_{COav(all\text{-}CO)} - \nu_{COav(PR3\text{-}coordinated)}$ and $\Delta E = E_{pc1(all\text{-}CO)} - E_{pc1(PR3\text{-}coordinated)}$.

complexes reported so far. As expected, only small cathodic shifts, ca. 30 mV for **2** and 60 mV for **3**, were observed for the Fe^IFe^I/Fe^0Fe^I reduction potentials in comparison to that of the all-CO diiron complex **1**,[36] indicating the exceptionally weak donating property of the $P(Pyr)_3$ ligand in comparison with that of other previously reported PR_3-coordinated analogues, which is in accord with the results of IR spectra. It is already known that $Ru(bpy)_3^{2+}$ displays three reversible reduction peaks for three bipyridyl ligands in the cyclic voltammogram with the reduction peak for $Ru(bpy)_3^{2+}/Ru(bpy)_3^{+}$ at –1.61 V ($E_{1/2}$). Therefore, the one electron reduction processes of **2** and **3** by the photogenerated $Ru(bpy)_3^{+}$ are thermodynamically feasible. The ΔE values listed in Table 1 show that the reduction potentials of all the previously reported diiron dithiolate complexes are much more negative than that of the corresponding $P(Pyr)_3$-coordinated diiron dithiolate complexes, so that the electron transfer from $Ru(bpy)_3^{+}$ to the other PR_3-coordinated diiron complexes is thermodynamically unfavorable.

Flash Photolysis. The kinetic feasibility for photoinduced electron transfer processes of the three-component systems was studied by laser flash photolysis. We have previously demonstrated that complex **1** could be reduced by $Ru(bpy)_3^{+}$, resulting in the formation of Fe^0Fe^I species with three characteristic absorptions at 400, 580, and 700 nm in the transient absorption spectrum.[36] To get high-quality transient absorption spectra for the electron transfer processes of $Ru(bpy)_3^{+}$ to complexes **2** and **3**, we first used dtc$^-$ as electron donor. The transient absorption spectrum at 0.2 μs after laser excitation (532 nm, pulse width 7 ns) of the deoxygenated solution of $Ru(bpy)_3^{2+}$, complex **2**, and dtc$^-$ clearly shows the absorption of $Ru(bpy)_3^{+}$ at 520 nm, which decays completely at 10 μs. At the same time the absorptions at ca. 390 and 520 nm, attributed to the one-electron reduced species of **2**, appear in the spectrum (Figure 1). The Fe^0Fe^I species of **2** does not display an apparent absorption at 700 nm, which is different from what we found for all-CO diiron complexes. Compared to the lifetime (τ = 17 μs) of $Ru(bpy)_3^{+}$ in the absence of **2**, the lifetime of $Ru(bpy)_3^{+}$ was shortened to 2.6 μs upon addition of **2** (0.2 mM). The concomitant kinetics for the decay of $Ru(bpy)_3^{+}$ at 520 nm and the buildup of the Fe^0Fe^I species at 400 nm further supports the conclusion that one electron transfers from $Ru(bpy)_3^{+}$ to **2** (Figure 1 inset). Efforts were made to obtain the characteristic transient absorptions of the one-electron reduced species of **3**, but the slow decay of $Ru(bpy)_3^{+}$ thwarted the observation of the absorption change in the range of 500−700 nm. However, the newly generated absorption for the one-electron reduced species of **3** could be clearly observed at 400 nm (Supporting Information, Figure S1). The lifetime of $Ru(bpy)_3^{+}$ was shortened to 7.2 μs upon addition of **3** (0.15 mM, Supporting Information, Figure S1). By varying the concentration of the diiron complexes, the rate constant of the electron transfer reaction from $Ru(bpy)_3^{+}$ to the Fe^IFe^I species is determined to be 3.5×10^9 M^{-1} s^{-1} for **1**, 2.0×10^9 M^{-1} s^{-1} for **2**, and 6.7×10^8 M^{-1} s^{-1} for **3**. It is noteworthy that the electron transfer rate constant greatly decreases as the number of $P(Pyr)_3$ ligands in the diiron complex increases. The cathodic shift of the reduction potential caused by CO-displacement makes the desired electron transfer less preferred.

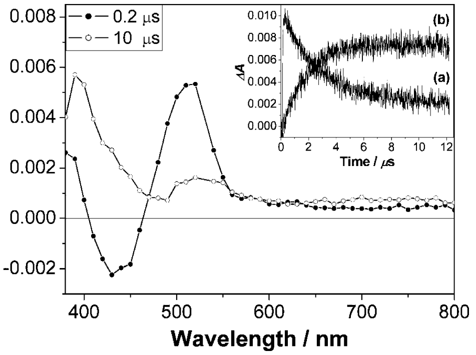

Figure 1. Transient absorption spectra obtained at 0.2 μs and 10 μs following laser flash photolysis of a deoxygenated CH_3CN solution containing $Ru(bpy)_3^{2+}$ (0.03 mM), dtc$^-$ (1.0 mM) and **2** (0.2 mM). Inset: kinetic traces at 520 nm (a) and 400 nm (b).

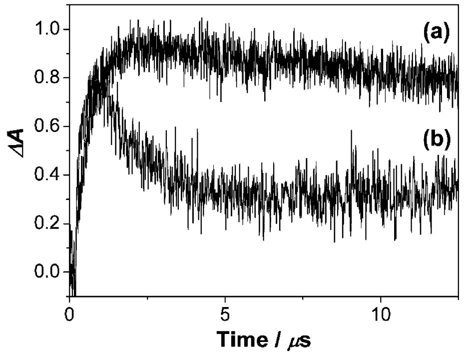

Figure 2. Kinetic traces at 520 nm obtained following flash photolysis of a deoxygenated mixture of CH_3CN/H_2O (1:1, v/v) containing (a) 0.03 mM $Ru(bpy)_3^{2+}$, 0.1 M H_2A; (b) the same as mixture a but with 0.2 mM complex **2**. The two decay curves are normalized for comparison.

When dtc$^-$ was replaced by H_2A, the lifetime (16.9 μs, curve a in Figure 2) of $Ru(bpy)_3^{+}$ was shortened to 1.9 (curve b in Figure 2) and 13 μs (Supporting Information Figure S2), respectively, upon addition of **2** and **3** (0.2 mM). The results indicate that electron transfer reactions from $Ru(bpy)_3^{+}$ to $P(Pyr)_3$-substituted diiron complexes are still feasible when H_2A is employed as electron donor under the condition for photochemical H_2 evolution.

Photochemical Hydrogen Production. After photoinduced electron transfer processes of the three-component systems were verified by laser flash photolysis, light-driven

Table 2. Effect of the CH_3CN/H_2O Ratio on Photochemical H_2 Evolution[a]

CH_3CN/H_2O (v/v)	H_2 evolved (μmol)	turnovers based-on cat.[b]	turnovers based-on PS[c]
3:7	13	1.3	26
1:1	43	4.3	86
7:3	19	1.9	38

[a] Reaction conditions: $Ru(bpy)_3^{2+}$ (0.1 mM), **2** (1.0 mM), and H_2A (0.1 M) in the solution of different CH_3CN/H_2O ratios, 3 h. [b] cat. = complex **2**. [c] PS = $Ru(bpy)_3^{2+}$.

Table 3. Effect of H_2A Concentration on Photochemical H_2 Evolution[a]

concentration of H_2A	H_2 evolved (μmol)	turnovers based on cat.[b]	turnovers based-on PS[c]
0.05 M	29	2.9	58
0.1 M	43	4.3	86
0.2 M	33	3.3	66
0.3 M	31	3.1	62

[a] Reaction conditions: $Ru(bpy)_3^{2+}$ (0.1 mM), **2** (1.0 mM) and different concentrations of H_2A in a 1:1 CH_3CN/H_2O solution, 3 h. [b] cat. = complex **2**. [c] PS = $Ru(bpy)_3^{2+}$.

hydrogen generation was studied. The reaction conditions for photochemical hydrogen production were optimized with complex **2** as catalyst. When the ratio of CH_3CN/H_2O was changed from 1:1 (v/v) to 3:7 and then to 7:3, the amount of H_2 generated in 3 h was reduced to ca. 30–44% of that evolved from a 1:1 CH_3CN/H_2O solution (Table 2). Presumably, it mainly results from the poor solubility of the diiron complex in the 3:7 CH_3CN/H_2O solution and, in a reverse case, from inefficient dissociation of H_2A in the 7:3 CH_3CN/H_2O solution. When the concentration of H_2A was varied from 0.05 to 0.1 M, the total amount of the hydrogen evolved grew from 29 to 43 μmol in a 1:1 CH_3CN/H_2O solution (Table 3). Further increase in the H_2A concentration led to decrease in the hydrogen evolution. The same tendency was also observed with different solvents and H_2A concentrations using complex **1** as catalyst (Tables S1 and S2). Tables 2 and 3 show the photochemical hydrogen generation reactions that were made with 0.1 M H_2A in the 1:1 CH_3CN/H_2O solution.

The three-component system of $Ru(bpy)_3^{2+}$, diiron complexes **1**−**3**, and H_2A were then explored for photochemical hydrogen generation. The GC analysis of hydrogen formation as a function of reaction time for complex **2** shows that the amount of hydrogen evolved increases steadily and levels off after ca. 3 h with a 0.1 M concentration of H_2A in a 1:1 CH_3CN/H_2O solution (Figure 3). The initial slopes of hydrogen generation for three diiron complexes **1**−**3** were measured to be 1.7×10^{-7} mol/min for **1**, 6.7×10^{-7} mol/min for **2**, and 3.0×10^{-7} mol/min for **3** under conditions indicated in Figure 3. The total amount of hydrogen evolved is 4.3×10^{-5} mol with 4.3 turnovers based on **2** and 86 turnovers based on $Ru(bpy)_3^{2+}$ in a 3-hour photolysis. The amount of hydrogen evolved is 1.7×10^{-5} mol with 1.7 turnovers based on **3** and 34 turnovers based on $Ru(bpy)_3^{2+}$. The total amount of hydrogen evolved is 7.8×10^{-6} mol with 0.78 turnover based on complex **1**. The IR spectra showed that without irradiation diiron complexes did not decompose in the presence of ascorbic acid in CH_3CN/H_2O solution under nitrogen atmosphere. The IR monitoring showed that complex **1** was completely decomposed after ca. 1 h under irradiation, while the CO bands of complex **2** disappeared after ca. 2.5 h under irradiation. $P(Pyr)_3$-monosubstituted complex **2** showed much higher catalytic activity than **1** and **3**. These results indicate that CO-displacement by a relatively weak electron-donating phosphine ligand $P(Pyr)_3$ improves the photostability and catalytic activity of [2Fe2S] model complexes in photocatalysis reactions in a certain extent.

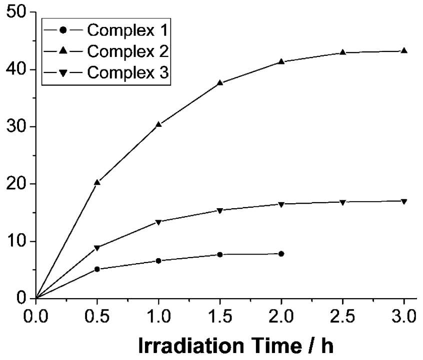

Figure 3. Reaction conditions: $Ru(bpy)_3^{2+}$ (0.1 mM), H_2A (0.1 M), and different diiron complexes (1.0 mM) in CH_3CN/H_2O (1:1, v/v).

Several control experiments were carried out to ascertain that the photoinduced hydrogen evolution was promoted by the [2Fe2S] model complex. As expected, hydrogen formation was not observed when the reaction of $Ru(bpy)_3^{2+}$, the diiron complex, and H_2A was carried out in the dark. Moreover, omission of any of the components of the three-component system did not generate detectable amount of H_2, suggesting that all three components are required in the H_2-producing process. The results of the control experiments indicate that the hydrogen generation in the present system is indeed photoinduced via the excited-state of $Ru(bpy)_3^{2+}$ and catalyzed by the [2Fe2S] model complexes.

Two other ruthenium polypyridine derivatives, $Ru(dmbpy)(bpy)_2^{2+}$ and $Ru(dmbpy)_3^{2+}$, were also used as photosensitizers to drive the electron transfer and hydrogen production with complex **2** as catalyst. As methyl groups were introduced to bipyridine rings, the redox potential for the $Ru(dmbpy)_3^{2+}/Ru(dmbpy)_3^{+}$ process is negatively shifted by ca. 100 mV in comparison to that for the $Ru(bpy)_3^{2+}/Ru(bpy)_3^{+}$ couple,[43] resulting in observable improvement of the electron-transfer rate constant. The rate constants for the electron transfer between $Ru(dmbpy)(bpy)_2^{+}$ and **2** and that between $Ru(dmbpy)_3^{+}$ and **2** were determined to be 2.0×10^9 and 2.5×10^9 M^{-1} s^{-1}, respectively. Although the rate constant for electron transfer from the photogenerated ruthenium complexes to the diiron complex is enhanced, the amount of hydrogen evolved slightly decreased with $Ru(dmbpy)(bpy)_2^{2+}$ as photosensitizer, and it significantly went down with $Ru(dmbpy)_3^{2+}$ as photosensitizer (Table 4). Considering that the potential for the $^*Ru(dmbpy)_3^{2+}/Ru(dmbpy)_3^{+}$ couple (0.23 V vs Ag/Ag^+ in CH_3CN/H_2O) is more negative than that for the $^*Ru(bpy)_3^{2+}/Ru(pby)_3^{+}$ couple (0.37 V) calculated according to the literature,[43] it could be predict that the electron transfer from the HA^- anion

---

(43) Juris, A.; Balzani, V.; Barigelletti, F.; Campagna, S.; Belser, P.; Zelewsky, A. *Coord. Chem. Rev.* **1988**, *84*, 85–227.

Table 4. Photochemical H_2 Evolution with Different Ru-Based Photosensitizers[a]

photosensitizer	H_2 evolved (μmol)	turnovers based-on cat.[b]	turnovers based-on PS[c]
$Ru(bpy)_3^{2+}$	43	4.3	86
$Ru(dmbpy)(bpy)_2^{2+}$	39	3.9	76
$Ru(dmbpy)_3^{2+}$	19	1.9	38

[a] Reaction conditions: H_2A (0.1 M) and **2** (1.0 mM) in a 1:1 CH_3CN/H_2O solution with different ruthenium complexes (0.1 mM), 3 h. [b] cat. = complex **2**. [c] PS = $Ru(bpy)_3^{2+}$, $Ru(dmbpy)(bpy)_2^{2+}$, $Ru(dmbpy)_3^{2+}$.

Scheme 2. The Proposed Photochemical Proton Reduction Processes Catalyzed by the Biomimetic [2Fe2S] Complexes

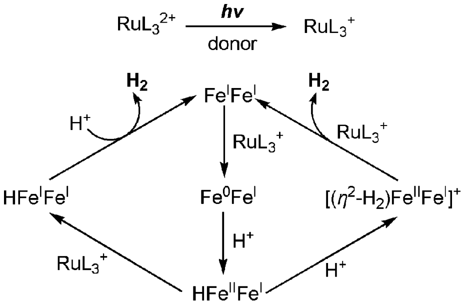

to $^*Ru(dmbpy)_3^{2+}$ is less favorable than to $^*Ru(bpy)_3^{2+}$. In light of the potential analysis, the decline in hydrogen evolution is attributed to the inefficient reductive quenching of the excited ruthenium photosensitizer by the ascorbate anion.

Discussion on the Mechanism. Although $Ru(bpy)_3^+$ is thermodynamically capable of reducing water to molecular hydrogen, the solution containing $Ru(bpy)_3^+$, formed by the reaction of H_2A and photoexcited $Ru(bpy)_3^{2+}$, does not produce detectable H_2 without catalyst.[11] Therefore, the proton reduction center can be attributed to the diiron dithiolate complex, which has been shown to be an effective catalyst for electrochemical reduction of protons to H_2.[20–30] A plausible process for photochemical hydrogen evolution is illustrated in Scheme 2. Upon irradiation with visible light, the photosensitizer $Ru(bpy)_3^{2+}$ is excited and then reduced to $Ru(bpy)_3^+$ by electron transfer from HA^-. The generated $Ru(bpy)_3^+$ is then capable of reducing the diiron complex to an Fe^0Fe^I species. Considering the reduction capability of $Ru(bpy)_3^+$ and the second reduction potentials of complexes **1**−**3** (−2.13 V for **1**, –2.16 V for **2**, and –2.20 V for **3**), further reduction of Fe^0Fe^I to Fe^0Fe^0 by $Ru(bpy)_3^+$ is thermodynamically unfavorable. In addition, protonation of the bridged-nitrogen atom of the diiron complex **2** was not detected by the IR spectrum in the presence of ascorbic acid (50 equiv) in CH_3CN/H_2O (3:1, v/v) solution. It therefore seems that there are two possibilities: (1) the Fe^0Fe^I complex is first protonated to give an $HFe^{II}Fe^I$ species which is then reduced to HFe^IFe^I. This new species should have sufficient hydride character to be protonated again to give H_2, and regenerating the Fe^IFe^I catalyst; (2) the $HFe^{II}Fe^I$ species first undergoes a second protonation to generate $[(\eta^2\text{-}H_2)Fe^{II}Fe^I]^+$ in accordance with the mechanism proposed earlier for electrochemical hydrogen generation catalyzed by the diiron dithiolate complexes.[23,24] The second protonation should render the reduction potential of the $[(\eta^2\text{-}H_2)Fe^{II}Fe^I]^+$ species positive enough to be reduced by $Ru(bpy)_3^+$, followed by release of H_2.

Conclusion

The strong reductant $Ru(bpy)_3^+$, generated from $Ru(bpy)_3^{2+}$ in the action of light, can transfer electrons to complexes **2** and **3** containing $P(Pyr)_3$ ligand(s) when the reductive quencher dtc^- was replaced by HA^-. Visible light-driven hydrogen evolution catalyzed by bioinspired [2Fe2S] complexes could be observed for the three-component system of $Ru(bpy)_3^{2+}$, [2Fe2S] complexes (**1**−**3**) and H_2A in a 1:1 CH_3CN/H_2O solution without requirement of extra proton acid. In comparison to the $P(Pyr)_3$-disubstituted complex **3** and the all-CO diiron complex **1**, the $P(Pyr)_3$-monosubstituted analogue **2** displays better photostability and improved catalytic activity in photochemical hydrogen generation. The total turnover numbers of 4.3 based on **2** and 86 based on $Ru(bpy)_3^{2+}$ in a 3-hour photolysis indicate that the photochemical hydrogen generation is catalytic both in the [2Fe2S] complex and in the photosensitizer $Ru(bpy)_3^{2+}$. Although the turnover number is low at this stage, the results illustrate the working principle, that is, bioinspired diiron complexes may act as economical catalysts for conversion of solar energy to a sustainable fuel, hydrogen gas.

Acknowledgment. This work was supported by the Chinese National Science Foundation (Grant Nos. 20471013 and 20633020), the Swedish Energy Agency, the Swedish Research Council, and K. & A. Wallenberg Foundation.

Supporting Information Available: Kinetic traces of the three-component system, $Ru(bpy)_3^{2+}$, dtc^-, and **3**; kinetic traces of the dyad system $Ru(bpy)_3^{2+}$ and H_2A, and of the three-component system $Ru(bpy)_3^{2+}$, H_2A, and **3**; tables for effect of the CH_3CN/H_2O ratio and the H_2A concentration on photochemical H_2 evolution using complex **1** as catalyst. This material is available free of charge via the Internet at http://pubs.acs.org.

IC702010W